Available online at www.sciencedirect.com
ScienceDirect
Journal of Power Sources 164 (2007) 782–791
JOURNAL OF POWER SOURCES
www.elsevier.com/locate/jpowsour

Investigation of the anhydrous molten Na–B–O–H system and the concept: Electrolytic hydriding of sodium boron oxide species

Daniel L. Calabretta [a,b,c,*], Boyd R. Davis [a,b,c]

[a] *Queen's-RMC Fuel Cell Research Centre, Kingston, Ont., Canada K7L 5L9*
[b] *Kingston Process Metallurgy, Inc., 1102 Lancaster Dr., Kingston, Ont., Canada K7P 2L7*
[c] *Department of Mining Engineering, Queen's University, 25 Union Ave., Kingston, Ont., Canada K7L 3N6*

Received 26 October 2006; received in revised form 19 November 2006; accepted 20 November 2006
Available online 18 December 2006

Abstract

Although sodium borohydride ($NaBH_4$) can act as an excellent hydrogen storage material, its cost renders it impractical for automotive applications. In this paper the concept of electrolytic production of $NaBH_4$ from sodium metaborate ($NaBO_2$) is introduced following a literature review of $NaBH_4$ synthesis. By deduction, we assert that only by employing dense solid oxide ion electrolytes and a molten salt solution containing the two constituents would such a process be possible. We investigated the molten anhydrous Na–B–O–H system by pressure differential thermal analysis (PDTA), X-ray diffraction (XRD) and gas evolution analysis (GEA) using the starting reagents sodium hydride (NaH), $NaBO_2$ and $NaBH_4$. We found that molten $NaBH_4$ is not stable with $NaBO_2$ above 600 °C due to the formation of sodium orthoborate ($Na_4B_2O_5$), hydrogen and boron. However, the quasi-reciprocal ternary system, (4/5)NaH–$NaBO_2$–(1/5)$NaBH_4$–(2/5)$Na_4B_2O_5$, that was discovered, proves that molten $Na_4B_2O_5$ is miscible and stable with molten $NaBH_4$ to at least 650 °C under the hydrogen pressures used in this study. As well, the compound $Na_6B_2O_5H_2$ was discovered and a substantial portion of the anhydrous Na–B–O–H phase diagram has been experimentally deduced. There is a large ionic liquid composition domain within the system that would allow for the electrolytic hydriding of sodium boron oxide species to be tested.

Keywords: Sodium borohydride; Regeneration; Hydrogen storage; Sodium hydride; Reciprocal system; Molten salts

1. Introduction

1.1. Hydrogen storage

The lack of a practical, affordable, and high energy density hydrogen storage method is a major barrier to the commercialization of hydrogen fuel cells (HFCs) for automotive applications. The energy densities for state-of-the-art liquefied or compressed molecular hydrogen storage systems cannot meet the 2015 energy density targets set by the USA Department of Energy (DoE) Freedom Car Program [1]. Liquid hydrogen has very low density (70.8 g l^{-1}) and requires a bulky cryogenic storage system, while compressed hydrogen (70 MPa) has even lower density and requires a heavy containment vessel [2].

The physisorption of hydrogen on activated, single-walled carbon nanotubes has been thoroughly investigated over the past decade. The energy required to release hydrogen bound to elements via Vander-Waals forces is low, limiting the possibility of storing useful quantities of hydrogen at near ambient temperatures, therefore, such hydrogen storage systems would have to be maintained at low temperatures (~77 K). Theoretical calculations, which are in agreement with experimental results, show that no more than 2 wt% H_2 can be absorbed on high surface area carbon [2], well short of the DoE's 2015 gravimetric energy density target (9 wt% H_2).

The most investigated reversible complex hydrides, sodium alanate ($NaAlH_4$) and magnesium hydride (MgH_2), cannot meet the DoE's 2015 energy density targets either, having 4.7 and 7.6 wt% H_2, respectively. Both require significant catalyst additions in order to desorb hydrogen with acceptable kinetics and are reactive towards moisture.

Some chemical hydrides, like sodium borohydride ($NaBH_4$), are candidate hydrogen storage materials that can meet the DOE's 2015 energy density targets. In this mode of hydrogen storage, complete oxidation (Eq. (1)) of the fuel occurs by way of hydrolysis (Eq. (2)), followed by electrochemical oxidation

* Corresponding author. Tel.: +1 613 547 0116x237; fax: +1 613 547 8125.
E-mail address: daniel@kpm.ca (D.L. Calabretta).

0378-7753/$ – see front matter © 2006 Elsevier B.V. All rights reserved.
doi:10.1016/j.jpowsour.2006.11.023

of hydrogen (Eq. (3)).

$$NaBH_4 + 2O_2 \rightarrow NaBO_2 + 2H_2O \quad (1)$$

$$NaBH_4 + 2H_2O \rightarrow NaBO_2 + 4H_2 \quad (2)$$

$$4H_2 + 2O_2 \rightarrow 4H_2O \quad (3)$$

The theoretical maximum initial gravimetric hydrogen storage density of a $NaBH_4$ HFC system is very high ($4H_2/NaBH_4 = 21.3$ wt%), but could only be approached if the water required for hydrolysis is supplied from the HFC anode cathode manifold in stoichiometric amounts (Eq. (2)), and if the hydrolysis reactor is pressurized [3]. Most of the investigations of $NaBH_4$ hydrolysis have been with regards to base-stabilized solutions [4] containing $NaBH_4$ (3–7 wt% H_2). By exposing these solutions to catalysts, such as ruthenium, hydrogen can be released with good kinetics and conversion. The current commercial $NaBH_4$ synthesis process in the USA, the Schlesinger process (Eq. (4)), has production and wholesale costs of US$ 18 and 55 kg^{-1} [5], respectively, and therefore $NaBH_4$ is too expensive to be considered a commercial vehicular fuel.

$$H_3BO_3 + (1/2)CH_4 + 4NaCl + H_2O \rightarrow NaBH_4 + 3NaOH + (1/2)CO_2 + 2Cl_2 \quad (4)$$

Since there have been claims in the literature of electrochemical regeneration in aqueous solutions, it is important to first address this work and other processes for $NaBH_4$ synthesis from $NaBO_2$. Then, this is followed by a discussion of the theoretical requirements for the electrolytic reverse oxidation reaction (Eq. (1)). The nature of the molten $NaBO_2$–4NaH–$NaBH_4$ composition domain under moderate hydrogen pressures is then presented.

1.2. Electrolytic $NaBH_4$ production in aqueous and organic media

Cooper [6] claimed that dissolved $NaBO_2$ in caustic solutions could be electrolyzed (20–80% faradaic current efficiency) to $NaBH_4$ with low current densities (0.6–1.5 kA m^{-2}) by using hydrogen absorbing metals (Ni, Hg) as cathodes. Hale and Sharifian [7] claimed that $NaBH_4$ and a variety of quaternary ammonium and phosphonium borohydrides could be synthesized in a similar cell schematic as that given by Cooper. Their result claimed that 1 M NaOH solutions (10 wt% $NaBO_2$) could be electrolyzed with 20% faradaic current efficiency at a Raney nickel cathode. Negative results while trying to validate the patent literature were later obtained by Gyenge and Oloman [8] and in our own laboratory. In caustic solutions they attempted to electrolyze $NaBO_2$ using amalgamated copper, nickel, palladium, zinc, and Raney nickel electroplated on stainless steel. Porous cathodes made of nickel boride and Raney-Ni were also used in caustic solutions. In addition, the electrolysis of trimethylborate ($B(OCH_3)_3$) was attempted in the organic mediums ethylenediamine, mixtures of hexamethylphosphoramide and ethanol. None of their experiments yielded any detectable amount of $NaBH_4$, even though very similar conditions as those described in the patent literature were used, for prolonged periods of time. Gyenge and Oloman concluded that improper analysis of the solutions led the other researchers to believe that they had actually produced $NaBH_4$.

The initial fundamental studies of $NaBH_4$ electrochemical oxidation [9–11] indicated that it is a highly irreversible 7–8 electron process in aqueous media. The reason for the irreversibility is understood considering that only saline hydrides, a priori, can reduce boron oxide species to give alkaline metal borohydrides. But saline hydrides react with water to give hydrogen and hydroxides at ambient temperatures and will further react with hydroxides to give hydrogen and oxide ions at higher temperatures [12]. As well, saline hydrides are insoluble and reactive to non-polar and polar organic solvents, respectively, thus, organic media is also unsuitable for electrolytic $NaBH_4$ synthesis.

During commercial $NaBH_4$ production (Eq. (5)), the insoluble reagents, sodium hydride (NaH) and tri-methylborate ($B(CH_3O)_3$), react while dispersed in mineral oil (~290 °C), by way of mechanical agitation.

$$B(CH_3O)_3 + 4NaH \rightarrow NaBH_4 + 3NaOCH_3 \quad (5)$$

Other than the 'dispersion' method, all other $NaBH_4$ synthesis processes occur in inorganic media.

1.3. Inorganic $NaBH_4$ synthesis

The synthesis of $NaBH_4$ via the reaction between $NaBO_2$ and MgH_2 (Eq. (6)) has been demonstrated by Kojima and Haga [13]. Later, Li et al. [14] also investigated the anhydrous Mg–Na–B–O–H system with the intent of regenerating $NaBH_4$ from $NaBO_2$. The reaction is now known to be favourable above 400 °C under hydrogen atmospheres (0.1–7 MPa).

$$2MgH_2 + NaBO_2 \rightarrow 2MgO + NaBH_4 \quad (6)$$

Kojima et al. went on to describe a separation and thermal intensive process whereby $NaBH_4$ was synthesized from coke, water and $NaBO_2$ (Eq. (7)).

$$NaBO_2 + 2H_2O + 2C \rightarrow NaBH_4 + 2CO_2 \quad (7)$$

Alternatively, synthesizing MgH_2 from MgO can be achieved by mostly electrolytic means. Krishnan et al. [15] gave an excellent review of the history of electrolytic metal production from metal oxide molten salt systems using solid oxide electrolytes. They demonstrated that it is possible to obtain high purity Mg (100% faradaic current efficiency) with high current densities (>1 A cm^{-2}) by applying large overvoltages and stirring a MgO–MgF_2 flux at 1300 °C under argon. They employed a commercial YSZ membrane in contact with a carbon rod anode that was in contact with molten copper. Mg vapors were condensed out of the system and MgO could be continually added to the electrolytic cell. The electrolytic reduction and oxidation reactions are given by Eqs. (8) and (9).

$$Mg^{2+} + 2e^- \rightarrow Mg_{(g)} \quad (8)$$

$$O^{2-} + C \rightarrow CO_{(g)} + 2e^- \quad (9)$$

1.4. One-step reverse (electrolytic) $NaBH_4$ oxidation

Electrolytic $NaBO_2$ hydriding (reverse of Eq. (1)) will not be possible in a single electrolytic cell, because the electrolyte, which would be aqueous, must have hydride character, but hydride ions will reacts with water to give hydrogen and hydroxide ions. However, the production of $NaBH_4$ from $NaBO_2$ may be possible using molten salt solutions and solid ion electrolytes. A dense solid oxide ion electrolyte is required to act as a separation barrier, allowing for the removal of oxygen from the system while preventing the back reaction between oxygen and hydride species [16]. Furthermore;

- $NaBO_2$ must be soluble in molten $NaBH_4$, and the resulting system must be stable (from decomposition) in the temperature regime where low temperature solid oxide electrolytes have reasonable conductivities (~650 °C).
- The $NaBO_2$–$NaBH_4$ electrolyte cannot dissolve the solid oxide ion electrolyte.
- Hydrogen reduction (Eq. (10)), borate reduction (Eq. (11)) and oxide ion oxidation (Eq. (12)), would be the cathode, interface/solution and anode reactions, respectively.

$$4H_{(d)} + 4e^- \rightarrow 4H^-{}_{(d)} \quad (10)$$

$$BO_2{}^-{}_{(d)} + 4H^-{}_{(d)} \rightarrow BH_4{}^-{}_{(d)} + 2O^{2-}{}_{(d)} \quad (11)$$

$$2O^{2-}{}_{(d)} \rightarrow O_{2(g)} + 4e^- \quad (12)$$

Investigations of the reversible H/H^- redox couple were inspired by potential thermogalvanic cell applications (waste heat recovery) and for electrochemical investigations of hydrogen absorption at different metal surfaces. Thus, far, molten salt systems including: LiCl–KCl [17–21], LiBr–KBr–CsBr [22–24], LiCl–CsCl [20,21] and LiCl–KCl–CsCl [20,21], at their respective eutectic compositions, with dissolved LiH (0.02–5 mol%), between 498 and 610 °C, have been investigated by various electrochemical techniques under hydrogen/argon atmospheres.

No published studies on coupling hydrogen reduction (Eq. (10)) to the oxide ion oxidation reaction (Eq. (12)) by way of a solid oxide ion electrolyte–molten oxide/hydride salt were found, and, to our knowledge, the H/H^- redox couple has not been investigated in the molten 4NaH–$NaBH_4$ system. In fact, not a single electrochemical study of any molten salt system containing a fusible borohydride was found.

1.5. Molten $NaBH_4$ and its investigated molten salt systems

By thermal gravimetric analysis (TGA), Ostroff and Sanderson [16] studied the stability of $NaBH_4$ under 0.1 MPa H_2, N_2 and air. Under air, at 294 °C, $NaBH_4$ reportedly reacted with oxygen to form $NaBO_2$. Under H_2 and N_2, weight loss was not observed below 512 and 503 °C, respectively. Dymova et al. [25] went on to investigate the thermal stability of $NaBH_4$ by differential thermal analysis (DTA), and were the first to explicitly report its fusion, which occurs at ~505 °C (0.1 MPa H_2). H_2 reportedly evolves to a small degree at the fusion temperature, before decomposition (595 °C). Stasinevich and Egorenko [26] studied the decomposition of $NaBH_4$ between 0.1 and 1 MPa H_2 by pressure-DTA (PDTA). They determined an empirical relationship for the decomposition temperature of $NaBH_4$ as a function of pressure. All of the aforementioned studies indicate that $NaBH_4$ is a "reversible hydride".

Stasinevich et al. [27] went on to investigate the 4NaH–$NaBH_4$ system by PDTA (0.1 and 1 MPa H_2). Their investigation at 0.1 MPa H_2 showed that NaH decomposes at the eutectic temperature (~395 °C). At 1 MPa, H_2 evolved at 720 °C (i.e. the decomposition temperature of $NaBH_4$), showing that NaH is far more stable once in solution with $NaBH_4$. The Na^+/H^-, $BH_4{}^-$ binary system was not rigorously investigated under greater than 0.1 MPa H_2.

All three investigations by Kuznetsov et al. [28–30] of the NaOH–$NaBH_4$ system indicated that sodium boron oxide species are miscible with molten $NaBH_4$. In their initial DTA investigation [28] (0.1 MPa hydrogen), they assigned the highly exothermic, irreversible, H_2 evolving effect at 320–350 °C the stoichiometry given by Eq. (13). Their future investigations [29,30], whereby the evolved H_2 was measured and the resulting product was investigated by X-ray diffraction (XRD), caused them to assign a different stoichiometry (Eq. (14)).

$$2NaOH_{(d)} + NaBH_{4(d)} \rightarrow NaBO_{2(s)} + 2NaH_{(d)} + 2H_{2(g)} \quad (13)$$

$$4NaOH_{(d)} + NaBH_{4(d)} \rightarrow Na_3BO_{3(d)} + 4H_{2(g)} \quad (14)$$

Only two other studies of molten salt systems with $NaBH_4$ as a constituent have been reported [31,32]. Neither Kojima and Haga [13] or Suda and co-workers [14] discussed the fusion of $NaBH_4$, even though their synthesis investigations were above its fusion temperature. Therefore, it has been 30 years since the last investigation, at least knowingly, of a molten $NaBH_4$ system. By employing the analytical techniques of PDTA, XRD and gas evolution analysis (GEA), we have investigated the molten $NaBO_2$–4NaH–$NaBH_4$ composition domain to determine if one of the the conditions required for the electrolytic hydriding of $NaBO_2$ can be satisfied (Section 1.4).

2. Experimental

2.1. Reagents

$NaBH_4$ of greater than 99.5 wt% purity (Lot# 42Y3H07E) was donated by the Rohm and Haas Company and used without additional purification. NaH was derived from a NaH–mineral oil mixture (Acros Organics C.A.S. 7646-69-7) by vacuum filtration in an argon glove box. Toluene was used as the non-polar solvent, and vacuum filtration was done three times, using fresh solvent and a new filter each time. The resulting product was determined to be greater than >97 wt% NaH by gas evolution analysis and the XRD pattern did not indicate that significant impurities were present.

Anhydrous $NaBO_2$ was obtained by dehydrating 200 g of $NaBO_2{\cdot}4H_2O$ (Sigma SO251-500G, 99 wt%). $NaBO_2{\cdot}4H_2O$ was firstly heated to 160 °C it in a 1 l Pyrex kettle and held under vacuum (30 min). The product was then cooled, crushed

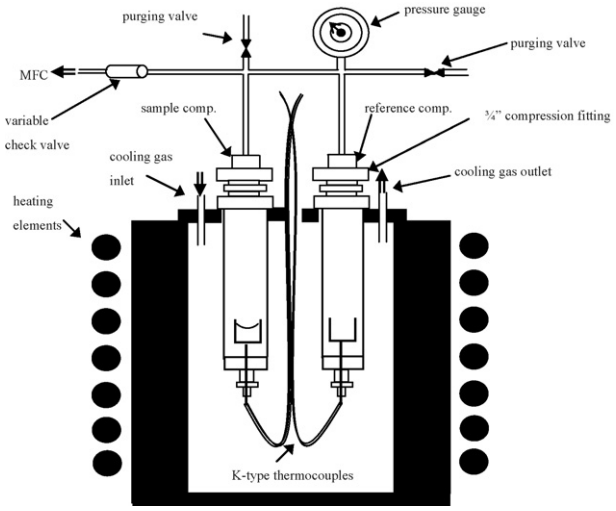

Fig. 1. Custom PDTA apparatus used during experimentation of the anhydrous Na–B–O–H system.

and reheated to 210 °C (vacuum, 3 h) before being cooled. Subsequent ball milling was done in a planetary ball mill under nitrogen atmosphere for a day. The product was then heated to 360 °C (vacuum) for several more hours. The final product was found to be 100% pure $NaBO_2$ by a standard titration procedure [33]. The XRD pattern did not indicate impurities.

2.2. PDTA apparatus construction

The custom PDTA apparatus (Fig. 1) used a custom 10 cm bore, 22 cm deep 120 V/15 A resistance furnace with Omega® CN4800 Series 1/16 DIN fuzzy logic temperature controller. The sample and reference compartments were constructed out of 16 cm × 19 mm o.d. SS 316 tubes (0.89 mm wall thickness). The bottoms of the compartments had 1.5 cm thick, 19 mm o.d. SS316 discs welded to them and 1.6 mm NPT to 1.6 mm Swagelok® SS316 bored through fittings were screwed into the bottom of the discs before they were welded shut. The compartment tops were fitted with 19 mm Swagelok® nuts and ferrules before placing them in a custom SS 316 lid that had inlet and outlet ports for purging gas (cooling). Stainless steel sheathed, 1.6 mm thick, 60 cm long K-type Omega® thermocouples were inserted through the bored-through 1.6 mm Swagelok® fittings such that the ends were 1 cm above the top of the welded metal disc. Nineteen millimetre o.d. SS 316 Swagelok® unions were compression-fitted to the top of the sample and reference compartments. 5 cm × 19 mm o.d. metal rods had 7 cm × 6.35 mm o.d. SS316 tubes welded into them and were compression-fit to the top of the unions. An Aalborg® GFM171 mass flow controller (MFC) with an accuracy of ±1.5% full scale (0–200 ml min^{-1}), was connected to a Swagelok® variable check valve. The rest of the apparatus consisted of a gas inlet and outlet, which allowed for the purging of the system. Data acquisition for temperatures and gas flow rates was achieved by employing an analog to digital interface (National Instruments® FP-1000), a personal computer and a program written in Labview®. Fieldpoint® modules (FP-TC-100 and FP-AI-110) were used to do the analog to digital conversion.

For each run, ∼5 g copper refrigeration caps (12.5 mm o.d.), which were first rinsed with 0.2 M HCl, followed by acetone, were used as sample crucibles. An empty copper crucible was used as the reference material.

The mass flow controller readings and differential heating curves (DHCs) were used to detect decomposition and thermal effect(s), respectively. The forthcoming experimentally deduced phase diagram was elucidated by differential heating curves (DCCs) exclusively, with a cooling rate of 4–6 °C min^{-1}. The onset temperatures of the DCCs have an accuracy of +6 °C due to thermal lag and undercooling. Much greater detail of the PDTA apparatus construction along with the initial studies of the anhydrous Na–B–O–H system is reported elsewhere [34].

2.3. Determination of hydride concentration

We tested the hydrogen concentration of equilibrated samples by gas evolution analysis, even if the MFC did not indicate decomposition, since it was possible that mild decomposition would be undetectable due to the accuracy of the flow meter. We constructed a GEA apparatus (Fig. 2) that closely resembles the one in the $NaBH_4$ digest [35]. Typically sample masses corresponding to 300 ± 100 ml of gas (STP) were employed for analysis. 0.5 M HCl was used to hydrolyze hydride compounds during analysis.

2.4. Phase identification

The microprobe-quenching technique cannot be employed for the determination of phases lying in the $NaBO_2$–$NaBH_4$–4NaH composition domain, since only one of the elements (sodium) can be detected and it is ubiquitous. Instead, a Panalytical® X'Pert Pro Multipurpose Diffractometer was employed to obtain XRD patterns after the samples had been

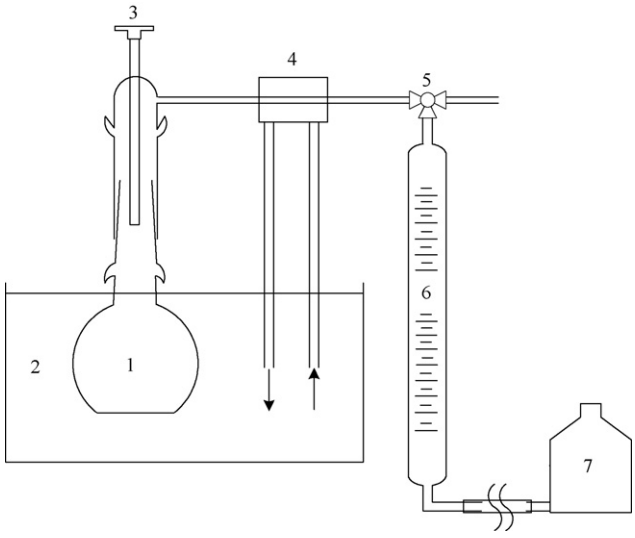

Fig. 2. GEA apparatus used to investigate hydride concentration after PDTA; 1, reaction flask; 2, water bath; 3, septum; 4, condenser; 5, three-way valve; 6, graduated cylinder; 7, confining solution.

analyzed by PDTA. This machine produces incident Co K α radiation by applying a 40 kV potential between the cathode and anode with a current of 45 mA. Samples were prepared for XRD analysis by one of two ways. The first involved taking preheated samples from the argon glove box and placing them on 32 mm o.d. borosilicate glass discs for analysis under normal atmospheric conditions, while the second way involved placing the crushed powders in 1 mm o.d. soft glass capillary tubes. The open ends of the capillary tubes were covered with paraffin and subsequently sealed with a propane torch moments after removing them from the argon glove box.

2.5. Analysis

For our initial investigations of the $NaBO_2$–4NaH–$NaBH_4$ composition domain, ~3 g samples were weighed into HDPE containers and mechanically shaken prior to being placed in copper crucibles (copper tubes welded into copper refrigeration caps). The samples were then placed in the sample compartment of the PDTA apparatus and partially sealed. The apparatus was compression-fitted immediately after it was removed from the glove box and then subsequently purged with >99.99 vol% H_2 by cycling the system from 0.2 to 1.2 absolute MPa 10 times (all pressures are given in absolute values). Samples were equilibrated at 530 °C (25 °C above the fusion temperature of pure $NaBH_4$) for 3 h, cooled and then crushed in the glove box using an agate mortar and pestle, before being analyzed for hydrogen content (GEA). PDTA (1.10 MPa) was then employed. Portions of the equilibrated samples were heated to decomposition. Knowing the decomposition temperature, subsequent cycling of the equilibrated sample, and in some cases, XRD under non-inert atmospheric conditions (Section 2.4) was done, to further analyze the compositions.

After becoming accustomed to the behaviour of the $NaBO_2$–4NaH–$NaBH_4$ system, the protocol was modified slightly. 0.3–0.5 g samples were directly weighed and mixed into their copper crucibles before heating them (PDTA 1.55 MPa) to 530 °C and allowing them to equilibrate for 30 min. The DCCs were recorded and the samples were crushed under argon before performing PDTA, cycling to a maximum temperature between 570 and 650 °C, followed by GEA and XRD (select compositions) under inert conditions (Section 2.4).

3. Results and discussion

3.1. $NaBH_4$–$NaBO_2$ system

Six 3 g (≤45 mol% $NaBO_2$) were analyzed by the protocol given in paragraph 1 of Section 2.5. During equilibration, the pressure in the apparatus did not increase and subsequent GEA indicated that 101.5 ± 4.5% of the initial hydrogen was present. While crushing the equilibrated samples, it was observed that there was an increase in the amount of non-dissolved material at the bottom of the crucible with increasing $NaBO_2$ concentration. 0.5–0.8 g of equilibrated sample from each of the six compositions were analyzed by PDTA (1.10 MPa) by heating them above the decomposition temperature of pure $NaBH_4$ (~720 °C). The onset temperatures of the endothermic effects (DHCs) and hydrogen evolution (MFC) are summarized in Table 1.

Table 1
PDTA (DHCs) effects of the $NaBO_2$–$NaBH_4$ system (1.10 MPa)

$NaBO_2$ (mol%)	DHC onset temperatures (°C)		
	I	II	III
5	512	610	730
10	500	620	710
15	506	596	713
20	519	610	722
25	503	610	726
45	505	596	

Effect I did not involve hydrogen evolution and began at the approximate fusion temperature of pure $NaBH_4$ (507.5 ± 8.5 °C), indicating that $NaBO_2$ is immiscible with $NaBH_4$. The onset temperatures (effects) II and III were taken from the mass flow controller and involved hydrogen evolution that occurred at approximately the same temperatures (608 ± 12 and 721.5 ± 8.5 °C), regardless of $NaBO_2$ concentration. The magnitude of hydrogen evolution increased (effect II) and decreased (effect III) with $NaBO_2$ concentration. From subsequent XRD analysis (Fig. 3) we found that the effects II and III are due to a reaction between the reagents (Eq. (15)) and $NaBH_4$ decomposition, respectively.

$$(3/2)NaBH_{4(l)} + (5/2)NaBO_{2(s)} \rightarrow 2B_{(d)} + Na_4B_2O_{5(d)} + 3H_{2(g)} \quad (15)$$

The FactSage® database indicates that the reaction (Eq. (15)) should be spontaneous at temperatures above 600 °C at standard pressure.

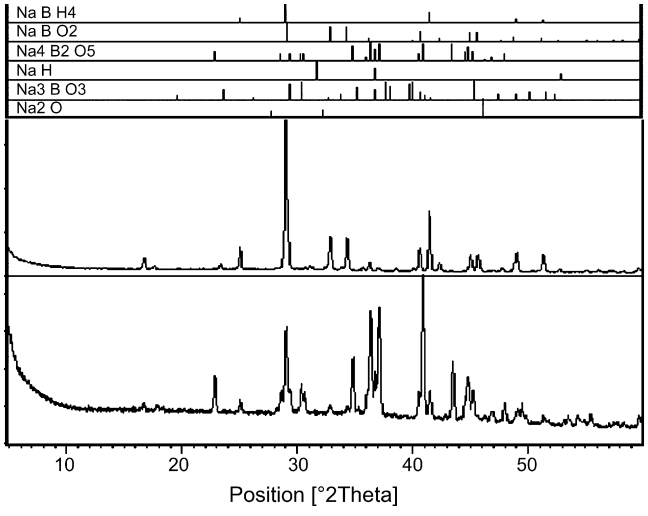

Fig. 3. XRD comparison of the initial $NaBO_2$ (45 mol%)–$NaBH_4$ system (1.10 MPa) after heating the system to below 535 °C (top) and above 650 °C (bottom) the hydrogen evolution reaction temperature.

Table 2
PDTA (DHCs) effects of the $NaBO_2$–4NaH–$NaBH_4$ system (1.10 MPa)

Na%	H%	DHC onset temperatures (°C)					NaH/$NaBO_2$
		i	ii	iii	iv	v	
28.2	94.7	380	426			731	3.17
26.0	95.2		430			740	1.10
28.2	83.9		433	478		735	1.05
28.2	73.1		431	476	647	721	0.63
28.2	62.7			479	658	736	0.45
26.0	85.2			474	611	722	0.36
28.2	52.3			487	662		0.36
28.2	73.1			479	626	722	0.21
28.2	62.7			478	634	741	0.15
28.2	52.3			474	634		0.12

3.2. $NaBO_2$–(4/5)NaH–(2/5)$Na_4B_2O_5$–(1/5)$NaBH_4$ quasi-ternary reciprocal system

Using the same protocol given in Section 3.1, analysis of 10 different compositions was done to investigate the effect of NaH addition to the $NaBO_2$–$NaBH_4$ system. Following equilibration, GEA gave 99.5 ± 3.5 mol% of the expected (initial) hydrogen. The onset temperatures for the endothermic effects (DHCs) and hydrogen evolution were obtained for equilibrated compositions (0.5–0.8 g) from their respective 3 g batches (Table 2). The onset temperatures were very dependent on the NaH to $NaBO_2$ ratio. Effect i occurred at a temperature similar to the eutectic of the 4NaH–$NaBH_4$ system (380 °C) but was only present for the composition with the highest NaH to $NaBO_2$ ratio (3.17). Effect ii was only present when the ratio was in excess of 0.63, and increased in magnitude as the ratio increased from 0.6 to 1.1. Effect iii was large and always present when the ratio was less than 1.05. Effect iv was a hydrogen evolving effect, which varied (635 ± 3.5 °C), and was only present when the ratio was less than 1.05. It is believed that effect iv is due to the same reaction given in Section 3.2 (Eq. (15)). Effect v also involved hydrogen evolution and is due, presumably, to $NaBH_4$ decomposition.

We identified the quasi-ternary reciprocal $NaBO_2$–(4/5)NaH–(2/5)$Na_4B_2O_5$–(1/5)$NaBH_4$ system by XRD analysis of compositions with low initial $NaBH_4$ concentration. The reaction (Eq. (16)) is believed to occur very rapidly above the 4NaH–$NaBH_4$ eutectic temperature. The FactSage® database indicates that the reciprocal reaction (Eq. (16)) is spontaneous over a large temperature range.

$$(4/5)NaH_{(d)} + NaBO_{2(s)} \rightarrow (1/5)NaBH_{4(d)} + (2/5)Na_4B_2O_{5(d)} \quad (16)$$

We employ the term quasi-ternary reciprocal, since three sodium cations are exchanged for a single boron cation during the reaction and the $NaBO_2$–(2/5)$Na_4B_2O_5$–$NaBH_4$ system does not dissolve $NaBO_2$ into solution before the hydrogen evolving reaction (Eq. (16)) occurs. The general Na–B–O–H reciprocal system, given by Fig. 4, illustrates the investigated compositions from this study. In addition, the compositions that we believe to have resulted following the irreversible hydrogen evolving reaction between NaOH and $NaBH_4$ in previous studies

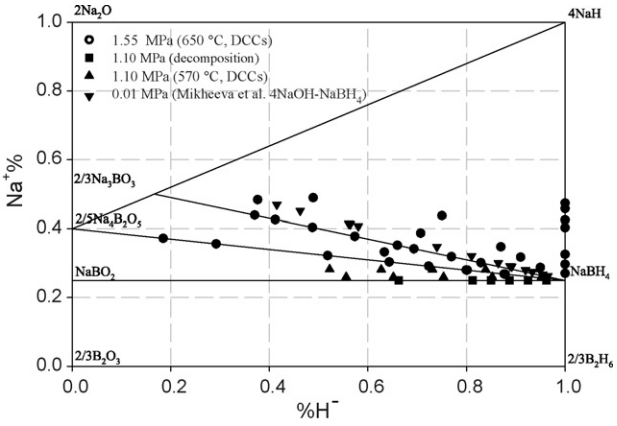

Fig. 4. Na–B–O–H ternary reciprocal diagram showing the investigated compositions during this study at 1.10 MPa (squares and triangles), 1.55 MPa (circles) and by Mikheeva and Kuznetsov [29] (inverted triangles).

[28–30] (the mechanisms of which will be discussed in Section 4), are also shown. We have tabulated the onset temperatures of the exothermic effects for the 10 compositions given in Tables 2 and 3 (rows 34–42), which were taken from DCCs after heating equilibrated samples from their respective 3 g batches to 570 °C.

3.3. (2/5)$Na_4B_2O_5$–4NaH–$NaBH_4$ composition domain

The protocol given in the second paragraph of Section 2.5 was used during the follow-up investigation of the (2/5)$Na_4B_2O_5$–4NaH–$NaBH_4$ composition domain. The reciprocal reaction (Eq. (16)) would not occur unless there was some $NaBH_4$ present in the initial mixture. For many of the investigated compositions, small quantities of gas (presumably hydrogen) evolved between 380 and 420 °C while heating them to the equilibration temperature. However, for samples that did not decompose below 650 °C, the hydrogen loss was too small to detect by subsequent GEA (97.5 ± 3%). Hydrogen evolution was most likely due to the reaction between hydride species and water or NaOH impurities in the initial reagents.

The effects given in row 4–7 (Table 3) were obtained from the first DCC for samples that were heated to 530 °C (equilibration) and the decomposition temperatures were taken from the MFC upon heating the sample a second time (to 650 °C). The effects given in rows 1–3 and 9–33 in Table 3 are the exothermic effects (DCCs) that were obtained following equilibration and subsequent heating of the samples to 650 °C.

Effect 1 is due to the liquidus of the molten (2/5)$Na_4B_2O_5$–4NaH–$NaBH_4$ composition domain. The compound $Na_6B_2O_5H_2$, was discovered (Eq. (17)) and effect 2 is due to the eutectic or cotectic of the $Na^+/B_2O_5^{4-}$, BH_4^- or $Na^+/B_2O_5H_2^{6-}$, $B_2O_5^{4-}$, BH_4^- binary and ternary systems, respectively. The $Na^+/B_2O_5^{4-}$, BH_4^- and $Na^+/B_2O_5H_2^{6-}$, BH_4^- binary systems, were experimentally determined (Figs. 5 and 6, respectively). The estimated eutectic compositions (extrapolation) and measured eutectic temperatures of the binary systems are 32.0 mol% (2/5)$Na_4B_2O_5$, 470 + 6 °C and 33.7 mol% (1/3)$Na_6B_2O_5H_2$, 425 + 6 °C, respectively. Effect 3 is the eutectic of the $Na^+/B_2O_5H_2^{6-}$, BH_4^- binary and the $Na^+/B_2O_5^{4-}$,

Table 3
Onset temperatures (°C) taken from DCCs (1.55 MPa)

H%	Na%	DCC onset temperatures (°C)					
		1	2	3	4	5	6
100.0	27.0	477			380		
100.0	29.7	441			383		
100.0	32.5	412			380		
100.0	40.3	445			382		618[a]
100.0	42.5	460			380		610[a]
100.0	45.8	483			380		590[a]
100.0	47.4	490			378		560[a]
95.0	28.8	450		424		376	
91.0	31.8			429		378	
87.9	26.8	467	458				
87.6	26.9	476	446	424			
87.0	34.7	460		411		380	
82.9	30.1	450		428			
80.2	28.0	467	458	428			
79.9	28.0	476	446				
77.0	31.9	432		426			
75.0	43.7	504				376	
72.3	29.1	468		429			
70.7	38.7	497		429		373	
69.4	34.2	433		427			
66.0	35.2	455		427			
64.4	30.4	487	474	426			
63.4	33.2	459		429			
57.3	37.8	475		427			
51.8	32.2	525	474				
48.9	48.9	517		425			
48.8	40.4	495		427			
41.2	42.6	499		425			
37.6	48.4	514		423			
37.0	43.9	505		427			
29.2	35.6	556	474				
18.5	37.2	569	473				
95.2	26.0	493	461	424			
94.7[b]	28.2	465		430		378	
85.2[b]	26.0	482	471				
83.9[b]	28.2	493	470				
75.4[b]	26.0	487	470				
73.1[b]	28.2	475		430			
65.2[b]	26.0	489	470				
62.7[b]	28.2	497	475				
55.6[b]	26.0	487	470				
52.3[b]	28.2	497	475				

[a] Taken from DHC while heating the system to 650 °C.
[b] Taken from DCCs after heating the compositions given in Table 2 to 570 °C (1.10 MPa).

$B_2O_5H_2^{6-}$, BH_4^- additive ternary systems. It is also the cotectic of the $Na^+/B_2O_5H_2^{6-}$, H^-, BH_4^- ternary system. Effects 4 and 5 are the eutectics for the Na^+/H^-, BH_4^- binary and the $Na^+/B_2O_5H_2^{6-}$, H^-, BH_4^- additive ternary systems, respectively. Compositions rich in $Na_6B_2O_5H_2$ were sulfuric yellow in color. The ternary behaviour in the $NaBH_4$ rich region of the $Na^+/B_2O_5^{4-}$, BH_4^- binary system (Table 3) was probably due to small concentrations of $Na_6B_2O_5H_2$ caused by the impurities water or NaOH (Eqs. (2), (13), (16), (17)). The behaviour was not observed while investigating compositions below the (2/5)$Na_4B_2O_5$–$NaBH_4$ composition line (Table 2) and we assume that the onset temperature of the cooling effects for

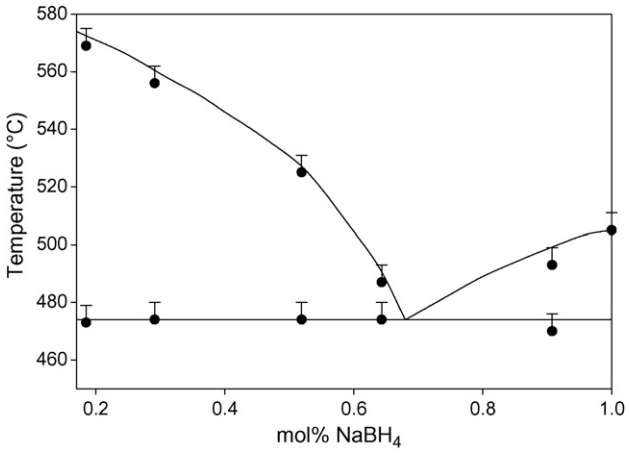

Fig. 5. Experimentally determined (2/5)NaB_2O_5–$NaBH_4$ phase diagram using the initial reagents $NaBO_2$, NaH and $NaBH_4$ (1.55 MPa).

the composition corresponding to the reciprocal diagram coordinates (83.9, 28.2) are due to $Na^+/B_2O_5^{4-}$, BH_4^- binary system, since, a priori, $NaBO_2$ is insoluble in the melt (Section 3.1). Concentrations rich in $Na_4B_2O_5$ had a muddy appearance at room temperature.

$$Na_4B_2O_{5(d)} + 2NaH_{(d)} \rightarrow Na_6B_2O_5H_{2(d)} \quad (17)$$

The eutectic temperature (effect 5) and composition that was measured and extrapolated (380 + 6 °C, 12.6 mol% 4NaH) for the Na^+/BH_4^-, H^- binary system (Fig. 7) was quite different than the ones reported (395 °C, 6.2 mol% 4NaH) by Stasinevich and Egorenko [26]. The difference is believed to be due to the decomposition of NaH, which they reported to occur above the binary eutectic temperature at 0.1 MPa H_2. For the pressure of this study (1.55 MPa), other than the small quantity of hydrogen that was evolved at the eutectic, the thermal effects upon cycling to 650 °C were reversible, with the exception of compositions >17.3 mol% 4NaH, which decomposed slowly below 640 °C, which is higher and lower than the measured decomposition temperatures of pure NaH (540 °C) and $NaBH_4$ (>720 °C), respectively. It was obvious when decomposition occurred since

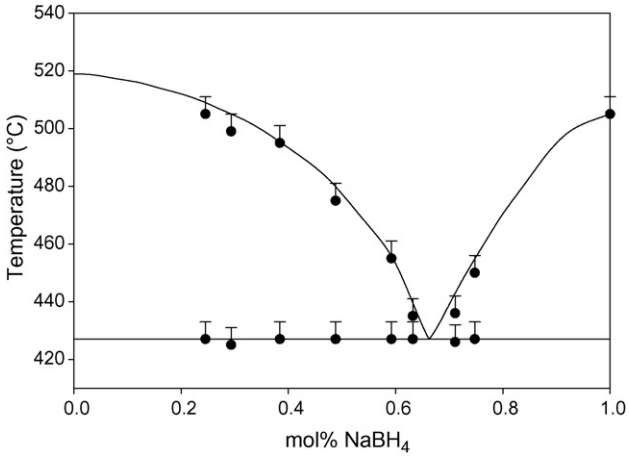

Fig. 6. Experimentally determined (1/3)$NaB_2O_5H_2$–$NaBH_4$ binary phase diagram using the starting reagents $NaBO_2$, NaH and $NaBH_4$ (1.55 MPa).

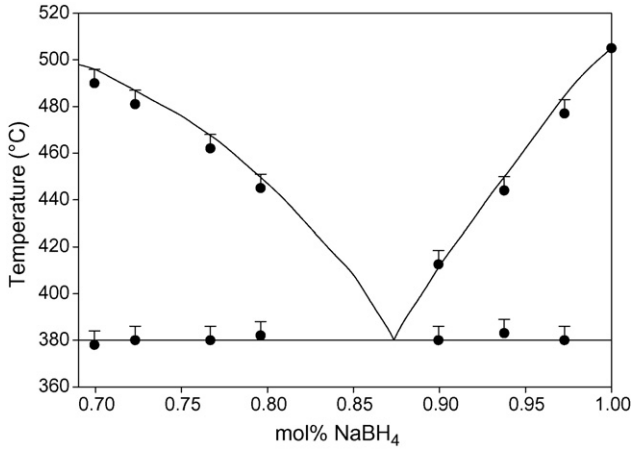

Fig. 7. Experimentally determined 4NaH–$NaBH_4$ binary phase diagram using the starting reagents $NaBO_2$, NaH and $NaBH_4$ (1.55 MPa).

the resulting samples were gum-like in texture, indicating the presence of sodium. The color of compositions in the Na^+/BH_4^-, H^- binary system that did not decompose were light grey at room temperature and substantial condensation was noticed after cooling, indicating that the hydride rich melts exhibit substantial vapor pressure above ~550 °C.

XRD patterns for compositions with the highest oxide concentration lying on the composition lines where the NaH to $NaBO_2$ mole ratios were 0.8, 1.6 and 4 are shown in Fig. 8. As well, the XRD pattern for the 4NaH(17.3 mol%)–$NaBH_4$ system that was heated to 610 °C is shown. The other known sodium boron oxide species [36–38], Na_3BO_3, Na_2O and $NaBO_2$ were not at all detectable by XRD, nor were the compounds Na_2O_2, or NaOH. We assume that the unidentified peaks are due to the $Na_6B_2O_5H_2$ compound.

In total, seven compositions lying within the (1/3) $Na_6B_2O_5H_2$–4NaH–$NaBH_4$ ternary region were analyzed by PDTA (Table 3). The ternary liquidus temperatures for these compositions indicate that the liquidus is quite steep while

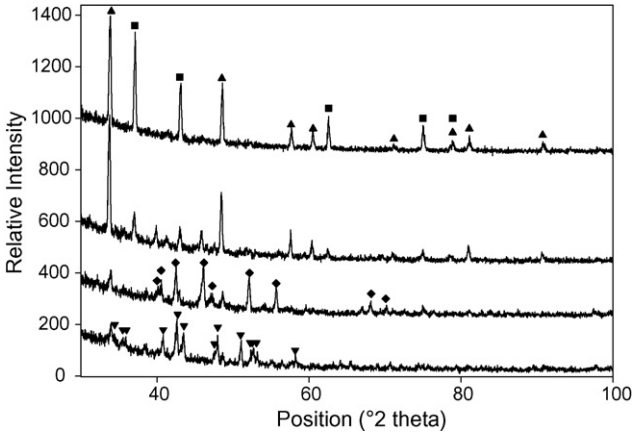

Fig. 8. XRD patterns of $NaBH_4$ (triangles); NaH (squares); $Na_4B_2O_5$ (upside down triangles); $Na_4B_2O_5H_2$ (diamonds); after heating composition using starting reagents $NaBO_2$, NaH and $NaBH_4$ corresponding to the Na–B–O–H reciprocal ternary composition domain coordinates (18.5, 37.2), (37.0, 43.9), (87.0, 34.7) and (1, 40.3), from bottom to top.

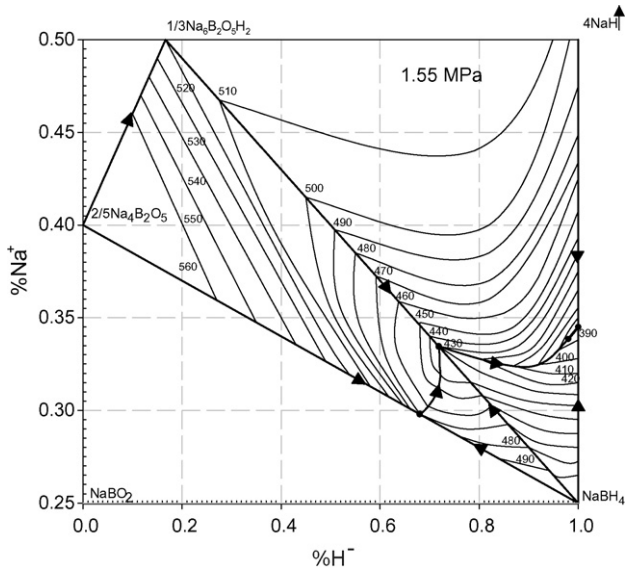

Fig. 9. Experimentally determined phase diagram using the starting reagents $NaBO_2$, NaH and $NaBH_4$ (1.55 MPa) of the (2/5)$Na_4B_2O_5$–4NaH–$NaBH_4$ composition domain lying within the anhydrous Na–B–O–H system.

moving towards 4NaH from the (1/3)$Na_6B_2O_5H_2$–$NaBH_4$ composition line. We estimate that the eutectic compositions of the $Na^+/B_2O_5H_2^{6-}$, H^- and $Na^+/B_2O_5^{4-}$, $B_2O_5H_2^{6-}$ binary systems to be near 100% $Na_6B_2O_5H_2$. We also estimate, by extrapolation, the melting temperature of $Na_6B_2O_5H_2$ to be 517 ± 5 °C. A substantial portion of the (2/5)$Na_4B_2O_5$–4NaH–$NaBH_4$ phase diagram has been experimentally deduced using the starting reagents $NaBO_2$, NaH and $NaBH_4$ (Fig. 9).

4. Further discussion

The results from the investigations of the NaOH–$NaBH_4$ system [28–30] (Section 1.5) could be explained by assuming that the overall reaction between the two constituents is equivalent to the coupling of Eq. (13) to the ternary reciprocal reaction (Eq. (16)), followed by the formation of $Na_6B_2O_5H_2$ (Eq. (17)). Our thermodynamic analysis using FactSage® indicates that the reaction given by Eq. (13), not Eq. (14), is highly exothermic, which is what was reported. The eutectic for the (1/3)$Na_6B_2O_5H_2$–4NaH–$NaBH_4$ additive ternary system, where the resulting compositions should have been lying (Fig. 4), was not reported, presumably due to the decomposition of NaH at the pressure of their study (0.1 MPa hydrogen). It is interesting to note that combining the NaH hydrolysis reaction (Eq. (18)) to Eq. (13) indicates that NaH is a catalyst to $NaBH_4$ hydrolysis above ~300 °C.

$$NaH + H_2O \rightarrow NaOH + H_2 \quad (18)$$

There is a wide range of compositions that could be used to test the solid oxide ion electrolyte approach to the electrolytic hydriding (Section 1.4) of either of the compounds $Na_4B_2O_5$ or $Na_6B_2O_5H_2$. However, it is evident that the electrolytic hydriding of $NaBO_2$ cannot be achieved, due to the immis-

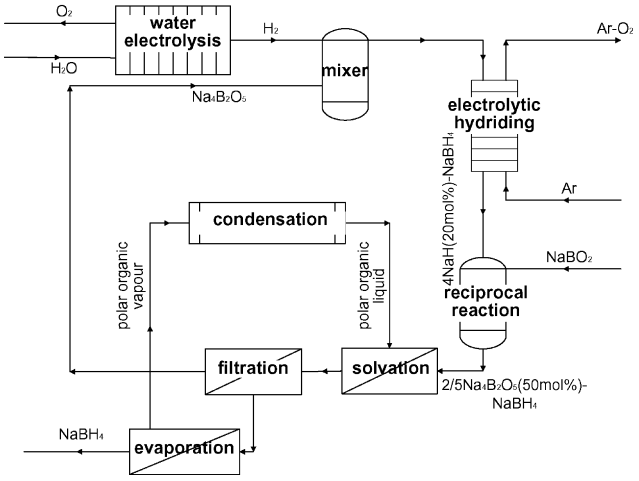

Fig. 10. The four major unit operations for the hypothetical hydriding of anhydrous $NaBO_2$ flow process.

cibility and instability of $NaBO_2$ with $NaBH_4$ at the desired temperature range (Section 3.1). At best, a four-unit operation flow-process including; water electrolysis, electrolytic hydriding (Eq. (19)), reciprocal reaction (Eq. (16)) and $Na_4B_2O_5$ separation (from $(2/5)Na_4B_2O_5$–$NaBH_4$ mixture(s)), could be considered (Fig. 10). If the electrolytic hydriding of pure $Na_4B_2O_5$ were possible, ideally, a 4NaH(20 mol%)–$NaBH_4$ mix would be used as a fuel in order to avoid two unit operations (reaction and separation). Such a fuel mix has a maximum 15 wt% H_2 (Section 1.1) and could be considered in situ with other proven hydrogen storage technologies, in particular, compressed hydrogen, to achieve the 2015 DoE energy density targets.

We have estimated the Gibbs energy of reaction for the electrolytic hydriding reaction (Eq. (19)) at 650 °C to be 820 kJ (4-electron, 2.12 V) by assuming an ideal solution model (FactSage®) for the Na^+/H^-, BH_4^- binary system and assuming that the enthalpy and entropy of fusion of NaH (melting temperature of 650 °C) to be the same as that of LiH. We also used our measured value for the enthalpy of fusion for $NaBH_4$ (15.1 kJ mol^{-1}), which we obtained using a TA Instruments® Q10 pressure differential scanning calorimeter (0.8 MPa H_2). The required thermodynamic data for $Na_4B_2O_5$ was taken from the FactSage® database. Multiplying our estimated Gibbs energy of reaction (Eq. (19)) by 1.3 (overpotentials) and adding it to the energy requirement for hydrogen production via high temperature (650 °C) water electrolysis (394 kJ for 2 mol H_2) multiplied by 1.2 (losses) and the theoretical energy required to heat 0.4 mol $Na_4B_2O_5$ and 2 mol of water from room temperature to 650 °C (239 kJ) multiplied by 1.1 (losses) gives a total energy requirement of 1849 kJ. Thus, our approximate estimate for the storage and production of 1 mol of hydrogen in the form of a 4NaH(20 mol%)–$NaBH_4$ mixture is 462 kJ. For comparison, the energy required to produce 4 mol of hydrogen by room temperature electrolysis, multiplied by 1.3 (losses), added to the energy required to liquefy or compress hydrogen is shown in Table 4. The calculated energy required to compress hydrogen has been determined from the Gibbs energy ($\Delta G = RT\ln(p_f/p_i)$)

Table 4
Energy requirement comparisons for the production (water electrolysis) and storage per mol of hydrogen

Storage mode	Energy (kJ mol^{-1} H_2)
4NaH(20 mol%)–$NaBH_4$[a]	462
Liquefaction[b]	419
Compression (68.9 MPa)[b]	320

[a] High temperature electrolysis (650 °C).
[b] Room temperature electrolysis.

and adding 5% of the theoretical value to account for the electrical losses, while the actual energy of liquefaction has been taken from a study [39]. Following the aforementioned assumptions, reverse oxidation of a 4NaH(20 mol%)–$NaBH_4$ mixture (Eq. (20)) would be a substantially more energy intensive process than that of the two modes of molecular hydrogen storage. However, to attain the vehicular goal of a hydrogen storage system with 9 wt% H_2, compressed hydrogen in situ with chemical hydride hydrolysis reactor, may be a plausible solution to hydrogen storage in terms of energy requirements, if electrolytic hydriding of sodium boron oxide species were possible.

$$2H_2 + (2/5)Na_4B_2O_5 \rightarrow (4/5)NaBH_4 + (4/5)NaH + O_2 \quad (19)$$

$$2H_2O + (2/5)Na_4B_2O_5 \rightarrow (4/5)NaBH_4 + (4/5)NaH + 2O_2 \quad (20)$$

Further speculation of potential flow-processes is unwarranted at this time since the electrolytic hydriding of $Na_4B_2O_5$ or $Na_6B_2O_5H_2$ has not been experimentally proven. A progressive follow-up study would be to investigate the stability of intermediate temperature solid oxide electrolytes in molten salts lying on the $(2/5)Na_4B_2O_5$–(4NaH (20 mol%)–$NaBH_4$) composition line (Figs. 4 and 9). Our preliminary investigation, which involved comparing PDTA cooling curves of relevant molten salt compositions with and without sintered LSGM discs being present, have been encouraging.

5. Conclusions

The newly discovered quasi-ternary reciprocal system, $NaBO_2$–$(4/5)NaH$–$(2/5)Na_4B_2O_5$–$(1/5)NaBH_4$, offers a new and perhaps improved mode of $NaBH_4$ synthesis. Moreover, the molten salt system(s) lying in the $(2/5)Na_4B_2O_5$–4NaH–$NaBH_4$ composition domain are very interesting, since they are stable from decomposition under moderate hydrogen pressures within the temperature rage where intermediate temperature solid oxide ion electrolytes have commercially acceptable conductivities.

Acknowledgments

The monetary support received from Kingston Process Metallurgy, AUTO21, DaimlerChrysler, NSERC, and IRAP are all gratefully acknowledged. As well, the council we received from

P. Coursol and A. Pelton during the course of the investigation was most useful.

References

[1] http://www1.eere.energy.gov/vehiclesandfuels/pdfs/program/hydrogen_storage_roadmap.pdf.
[2] A. Zuttel, Mater. Today 6 (2003) 24–33.
[3] Y. Kojima, Y. Kawai, H. Nakanishi, S. Matsumoto, J. Power Sources 135 (2004) 36–41.
[4] Q. Zhang, G. Smith, Y. Wu, R. Mohring, Int. J. Hydrogen Energy 31 (2006) 961–965.
[5] Y. Wu, U.S. Department, Annual EERE Progress Report, 2003.
[6] B.H. Cooper, US Patent 3,734,842.
[7] C.H. Hale, H. Sharifan, US Patent 4,931,154.
[8] E.L. Gyenge, C.W. Oloman, J. Appl. Electrochem. 28 (1998) 1147–1151.
[9] R.L. Pecsok, J. Am. Chem. Soc. 75 (1953) 2862–2864.
[10] J.P. Elder, A. Hickling, Trans. Faraday Soc. 58 (1962) 1852–1864.
[11] J.A. Gardiner, J.W. Collat, Inorg. Chem. 4 (1965) 1208–1212.
[12] Q. Xu, R. Wang, T. Kiyobayashi, N. Kuriyama, T. Kobayashi, J. Power Sources 155 (2006) 167–171.
[13] Y. Kojima, T. Haga, Int. J. Hydrogen Energy 28 (2003) 989–993.
[14] Z.P Li, B.H. Zhu, N. Morigasaki, S. Suda, J. Alloys Compd. doi:10.1016/j.jallcom.2006.07.119.
[15] A. Krishnan, X.G. Lu, U.B. Pal, Met. Mater. Trans. B 36 (2005) 463–473.
[16] A.G. Ostroff, R.T. Sanderson, J. Inorg. Nucl. Chem. 4 (1957) 230–231.
[17] H. Nakajima, T. Nohira, Y. Ito, Electrochem. Solid-State Lett. 5 (2002) E17–E20.
[18] T. Nohira, Y. Ito, J. Electrochem. Soc. 149 (2002) E159–E165.
[19] T. Murakami, T. Nishikiori, T. Nohira, Y. Ito, J. Electrochem. Soc. 150 (2003) A928–A932.
[20] H. Ito, Y. Hasegawa, Y. Ito, J. Electrochem. Soc. 149 (2002) E273–E280.
[21] H. Ito, Y. Hasegawa, Y. Ito, J. Electrochem. Soc. 150 (2003) E244–E250.
[22] T. Kasajima, T. Nishikiori, T. Nohira, Y. Ito, J. Electrochem. Soc. 150 (2003) E403–E408.
[23] T. Kasajima, T. Nishikiori, T. Nohira, Y. Ito, J. Electrochem. Soc. 150 (2003) E355–E359.
[24] T. Kasajima, T. Nishikiori, T. Nohira, Y. Ito, Electrochem. Solid-State Lett. 6 (2003) E5–E9.
[25] T.N. Dymova, N.G. Eliseeva, V.I. Mikheeva, Russ. J. Inorg. Chem. 12 (1967) 1223–1225.
[26] D.S. Stasinevich, G.A. Egorenko, Russ. J. Inorg. Chem. 13 (3) (1968).
[27] D.S. Stasinevich, G.A. Egorenko, G.N. Gnedina, Dok. Akad. Nauk SSSR 168 (1966) 610–612.
[28] V.I. Mikheeva, V.B. Breitsis, V.A. Kuznetsov, O.N. Kryukova, Dok. Akad. Nauk SSSR 187 (1969) 103–105.
[29] V.A. Kuznetsov, V.I. Mikheeva, Russ. J. Inorg. Chem. 15 (1970) 849–850.
[30] V.I. Mikheeva, V.A. Kuznetsov, Russ. J. Inorg. Chem. 16 (1971) 642–645.
[31] G.A. Egorenko, D.S. Stasinevich, Russ. J. Inorg. Chem. 13 (1968) 301–302.
[32] K.N. Semenenko, A.P. Chavgun, V.N. Surov, Russ. J. Inorg. Chem. 12 (1971) 271–272.
[33] R.S. Branan, Encyclopedia of Industrial Chemical Analysis, John Wiley and Sons, New York, 1986, pp. 384–423.
[34] D.L. Calabretta, Master's Thesis, Queen's University, January 2006.
[35] http://www.hydridesolutions.com/pdf/sodiumborohydridedigest.pdf.
[36] C. Wang, H. Yu, H. Liu, Z. Jin, J. Phase Equilib. 24 (2003) 13–20.
[37] G.W. Morey, H.E. Merwin, J. Am. Chem. Soc. 58 (1936) 2248–2254.
[38] T. Milman, R. Bouaziz, Ann. Chim. 3 (1968) 311–321.
[39] M. von Ardenne, et al., Effekte der Physik, Verlag Harri Deutsch, Frankfurt am Main, 1990, p. 712.